International Journal of Scientific Engineering and Applied Science (IJSEAS) – Volume-2, Issue-4, April 2016
ISSN: 2395-3470
www.ijseas.com

Monitoring dust at Cairo city from Aeronet data

Dr Eman Gaber Hamza
assistant Professor in Physics Physics Department University of Hail
Hail , Kingdom Of Saudi Arabia

Abstract. This study is based on an analysis of available meteorological data from ground stations an addition to AERONET data.. Number of severe dust storms, originating from western arid and desert regions , affect the whole during the season (March–May). Pronounced changes in the aerosol optical parameters, derived from AERONET, have been observed over Cairo University station(30°01\N, 31°.12\E) during period (2004–2005).Monthly average values of aerosol optical depth (AOD) showed a pronounced temporal trend, with a maximum AOD during winter and the transition season (spring) at two sites urban areas. Variation of Angstrom exponent α with the AOD was clear and the α value depends on the spectral range used in its determination. The data were compared against output from WRF model and meteorological observations.

1. INTRODUCTION

Dust emission is a serious environmental problem in arid and semi-arid region of Africa and Mediterranean area and in many other parts of the world. Strong wind erosion events such as sever dust storms, may threaten human lives and cause substantial economic damage. A lot of progress on the simulation of dust emission has been done. The first attempt to combine the information of the atmospheric data with land surface data for dust emission assessment was made by Gillette and Hanson (1989) in their investigation of the spatial and temporal variations of dust production.
Transport of desert dust is an important modifier of climate, through its effects on the following: backscattering and absorption of solar and terrestrial radiation (Miller and Tegen, 1998, 1999; Tegen et al, 1996), the heat budgets of the lower troposphere (Alpert et al., 1998) and the surface layers of the ocean (Schollaert and Merrill, 1998), especially in the case of semi enclosed seas (Gilman and Garrett, 1994).

We are concerned with quantitative prediction of dust storms in real time, with a focus on northeast Africa. There are two motivations for this work: (1) The arid and semiarid regions of the African desert are major sources of mineral dust which plays an important role in the global aerosol cycle. Hence the prediction of dust concentration and size characterization is an important issue in atmospheric research (e.g., Sokolik et al., 1998; Shao et al., 2003). (2) From spring to early summer, dust storms frequently occur in the east and northeast of Africa, including Egypt.

2. Batch Code for the Navy Aerosol Model

This program is called NAM6, which stands for Navy Aerosol Model, version 6. The batch program operates sequentially on each line of an input file.1 Each line of the input file (after the zeroth) contains a line index (which can be thought of as the time) followed by four numbers representing the values of each of the four NAM parameters. The zeroth line of the input file contains six control parameters. The first two of these are the optical

wavelength in **µ**m and the number of remaining lines in the file. Appendix A provides a sample input file with 10 input lines.
For each line of the input file, the program reads in the four parameters, computes the size distribution, and calculates, among other things, the optical extinction coefficient, β_{ext}, from the formula:

$$\beta_{ext}(\lambda) = \pi \int_0^{\infty} r^2 \frac{dN}{dr} Q_{ext}\, dr \quad Mm^{-1} \qquad (1)$$

In this equation λ (µm) is the optical wavelength,r (µm) is the radius of the spherical aerosol particle, and Q_{ext} (dimensionless) is the Mie efficiency factor for extinction. The Mie efficiency factor (van de Hulst, 1981) is the ratio between the optical and physical cross-sections of the particle. The Mie factors are computed in a subroutine called MIEV0 (Wiscombe, 1979) written by Warren J. Wiscombe and obtained from him via the Internet.

3. The properties of dust aerosol and reducing tendency of the dust storms in Egypt

Africa dust storms (ADS) are known to be a major air pollution source. ADS have strongly affected the environment of human beings in many as pacts: they interrupt the balance of radiation, accelerate the desertification and degrade the ecological system in Africa arid regions that are usually thought as the main sources of dust storms.
The effects of environment of ADS are causing concern world wide in the dry season, strong winds blow dust high into the atmosphere to form ADS, and westerly upper level winds bring fine dust from west to the east or southeast to form regional brown clouds. Estimated that about 800Tg of dust from Africa arid/semi-arid region (mainly from desert) are discharged into the atmosphere annually, which may be half of the dust generated around the world and have a great adverse influence on human health .Moreover, dusts floating in the air absorb and scatter solar radiation directly, altering regional radiation balance and affecting atmospheric stability, vertical motions, the large-scale circulation and hydrologic cycle, with significant regional climate effects .
The recent images from the satellites showed that the radius of cloudy droplet is much smaller over land than over ocean, for the reason that the aerosols with high density over land compete with air moisture, making it difficult to form rain. This phenomenon is explained as the effect of air dust on rain formation. Therefore ADS have played an extremely important role in climatology, weather forecasting, and biogeochemical cycling. Since the sources of ADS have all been found in remote areas, few observational data are available for research. Many of their characteristics remained unknown. It is necessary to investigate properties of ADS in source area so we can evaluate the influence of ADS on human beings and their environment more accurately.
Desert is one of the most important sources of ADS. Most of the desert is in west of Cairo. There are about 54 weather stations around this area. The routine work of those weather stations was to record dust storms when storms came and the recorded data included starting time, duration, atmospheric visibility, maximum wind speed and direction, humidity and precipitation. These data are very simple, but recorded for a long period, 37 years. Starting from late 1998 a number of new observations on dust aerosols have been carried out with the help of advanced equipment in Cairo Weather Station (lat:30°.01′33″N, long: 31°.12′25″E), the closest station to western Desert .The observations include the mass density of dust over the ground, scattering coefficient, visibility and aerosol optical depth. The combination of these advanced measurements and the long-term climate data allow a better characterization of ADS.

International Journal of Scientific Engineering and Applied Science (IJSEAS) – Volume-2, Issue-4, April 2016
ISSN: 2395-3470
www.ijseas.com

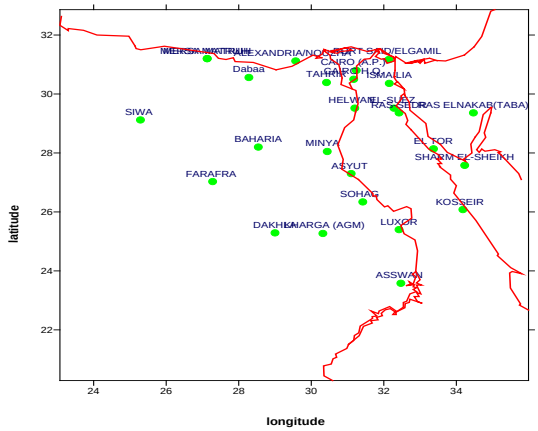

Fig. (4.1). Geographical location of Cairo Weather Station and the other weather stations with ADS observations.

The purpose of our work is to analyze mass concentration of dust aerosol and its variation for both ADS weather and clear days in Cairo, to understand the radiative effect of ADS, and to describe the temporal and spatial distribution of the intensity of ADS in the past 37 years in

4. Data analysis method

The temporal variation of dust aerosol mass concentration and the tendency of the intensity of dust storm in Cairo

According to guidelines, set by the Egypt Meteorological Observations, a dust storm is recorded when the horizontal visibility at the ground is < 1 km in dust weather with the instantaneous wind speed > 10 ms^{-1}. From January 2001 to December 2003, there were a total of 84 dust storms that occurred in Cairo and its surroundings (Table 4-1).

Table 4-1

Information about beginning time and duration of each dust storm from January 2001to December 2003 in Cairo

2001			2002			2003		
date	time[a]	durati	date	time[a]	dura	date	time[a]	duration[b]
2-JAN	12	3	24-FEB	1	5	28-JAN	15	2
3-FEB	9	10	11-MARS	16	4	3-FEB	9	2
20-FEB	11	3	23-MARS	11	4	7-FEB	15	9
23-MARS	13	9	26MARS	6	6	8-FEB	15	3
31-MARS	11	7	31-MARS	11	6	9-FEB	16	9
18-APRIL	14	6	18-APRIL	14	6	20-FEB	16	3
23-APRIL	5	6	5-APRIL	11	8	18-MARS	17	7
30-APRIL	9	11				25-MARS	12	2
6-MAY	9	8				2-APRIL	11	9
12-MAY	15	6				29-MAY	6	7
13-MAY	2	10						
2-DEC	13	5						

a Time: the beginning time of a dust storm in local solar time.

b Duration: the duration of a dust storm in minutes.

The maximum duration of the dust storm was >9h, on 30 April 2004;the minimum was about 2 h, and the average was 6h during this 3 year period (Table 4-2). The average of the data measured in dust storms and clear days in 3 years is shown in Table2. The maximum frequency of dust storms occurred in April, which accounted for 23% of overall

occurrences. There were no dust storms in the fall season (Jan, July), and in early winter months (October, November).

Table (4-2)

Average value of the data in dust storms and in clear days from 2004 to 2005 measured in Cairo

Measurements	In dust storms	In clear days
Mass density of air (mg m^{-3})	2.50 ± 2.12	0.10 ± 0.05
Wind speed (m s^{-1})	11.27 ± 1.85	2.6 ± 1.60
Visibility (km)	2.08 ± 1.03	16.19 ± 11.22
Scatter coefficient (M m^{-1})	2385.76 ± 2327.55	209.68 ± 180.70
Aerosal optical depth	3.06 ± 1.68	0.25 ± 0.20
Ångström exponent index	0.32 ± 0.09	2.13 ± 0.55
Average duration of a dust storm (min)	120.60 ± 87.74	

Fig. (4.2) provides the monthly average mass concentration of dust aerosol for dust storms from 1968 to 2004. The variation of the monthly average of mass concentration was from about 1.14 to 5.04 mgm^{-3} in dust storms and from 0.10 to 0.38 mgm^{-3} in clear days. Station and it can be calculated by regular data.

. In order to analyze the tendency of dust storms over the past 37 years, we define the IIDS to describe the intensity of a dust storm recorded weather.

The definition of IIDS is the following:

IIDS = nut / NŪT

N is the total number of weather stations in a radius of 400km from the recorded station; n is the number of the stations which also recorded the

dust storm in the same time ($n \leq N$);); u and Ū are the wind speed in the dust storm and the average wind speed of the total dust storms, respectively (ms^{-1}); t and T are the duration in minutes of the dust storm and the average duration of the total dust storms.

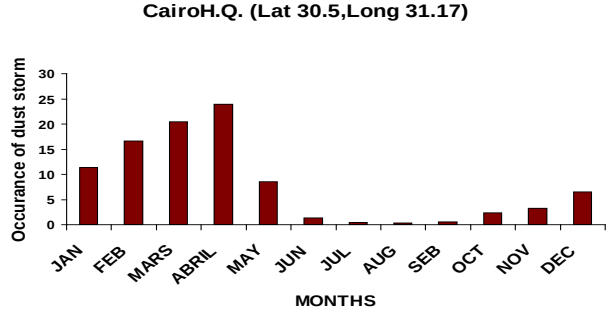

Fig. (4.2):- provides the monthly average mass concentration of dust aerosol for dust storms from 1968 to 2004

The IIDS values are accumulated for an entire year to form **TIIDS (total of IIDS in one year), a quantity that describes the annual intensity of dust storms for a particular location.

International Journal of Scientific Engineering and Applied Science (IJSEAS) – Volume-2, Issue-4, April 2016
ISSN: 2395-3470
www.ijseas.com

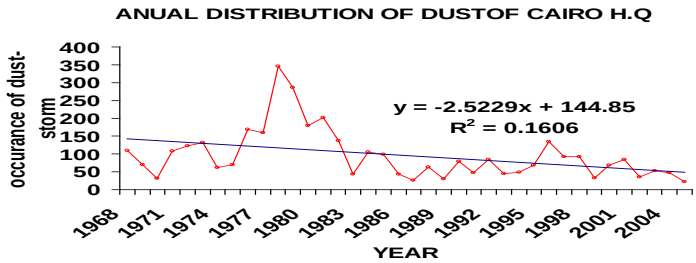

Fig.(4.3):- the temporal variation of TIIDS in Cairo.

Fig.(4.3) shows the temporal variation of TIIDS in Cairo, there is a large scatter in TIIDS and the trend of TIIDS was Decreasing (Fig. 4.3) in Cairo, especially in the past 37 years. This decreasing trend has also been identified.

4-3.3. Spatial distributions of various types of dust storm events in all of Egypt

It has statistically been analyzed that the data came from all monthly occurrence days of dust storm events, which were derived from 25 meteorological observing stations in Egypt during 1968–2004. And the spatial distribution charts (Fig. 4.1) have been drawn. The spatial distribution of 37 year average (1968 to 2004) is presented in Fig. (4.7), which represents the activities of the dust storms in Egypt. The dust storms were active in Sahara and transported to Cairo by strong south western dry winds (Khamsin events). The value of CACHE were higher in both the desert and near by areas where The distributions of dust sources play an important role in the formation of dust storms.

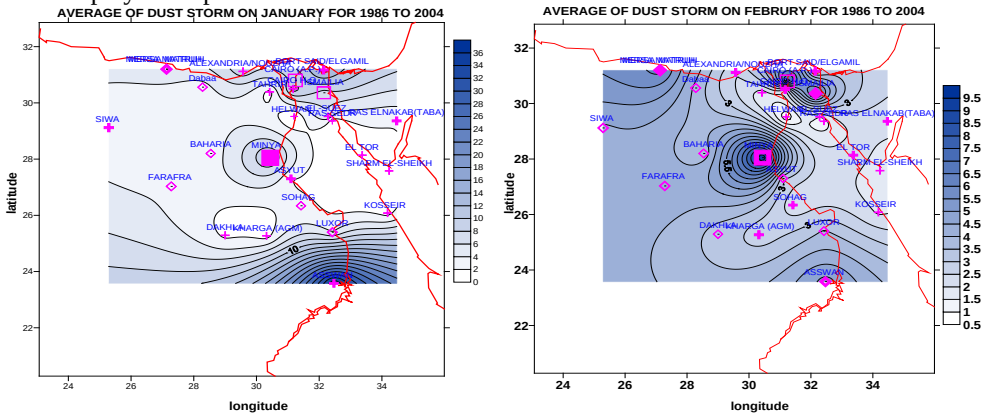

International Journal of Scientific Engineering and Applied Science (IJSEAS) – Volume-2, Issue-4, April 2016
ISSN: 2395-3470
www.ijseas.com

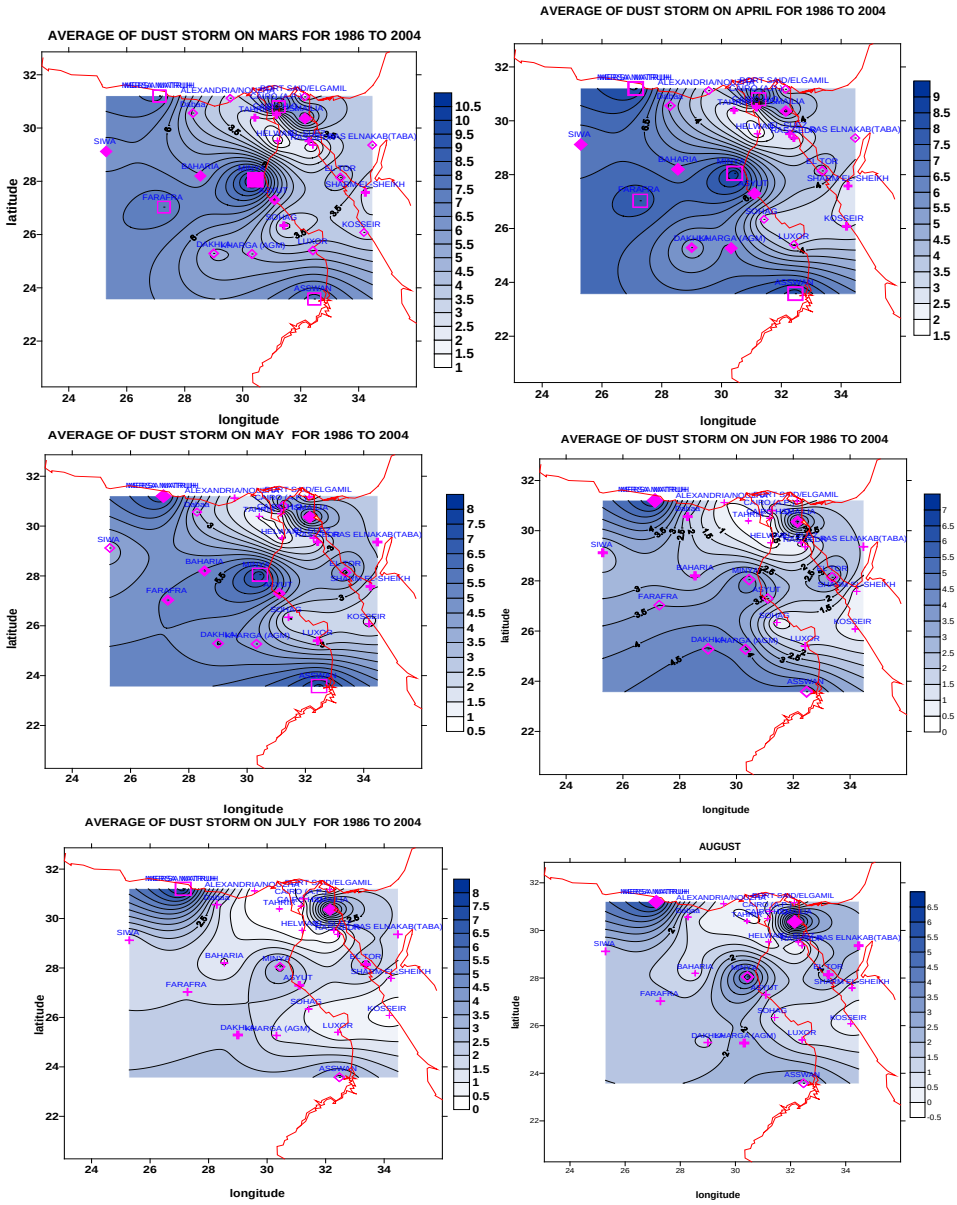

Fig. (4.8). The average of dust storm on Egypt for 1968 to 2004.

Fig.(4.8) also indicates that the areas where 37-year mean annual occurrence days of dust storms are more than 10 hours are located in South Minya, Dakhl, Kharga, Asyut stations and weastern Farafra,Baharia, which all near the desert. In addition, the spatial distribution range of blowing dust extended eastwards noticeably to Northeast Egypt and the East Egypt Plain.

International Journal of Scientific Engineering and Applied Science (IJSEAS) – Volume-2, Issue-4, April 2016
ISSN: 2395-3470
www.ijseas.com

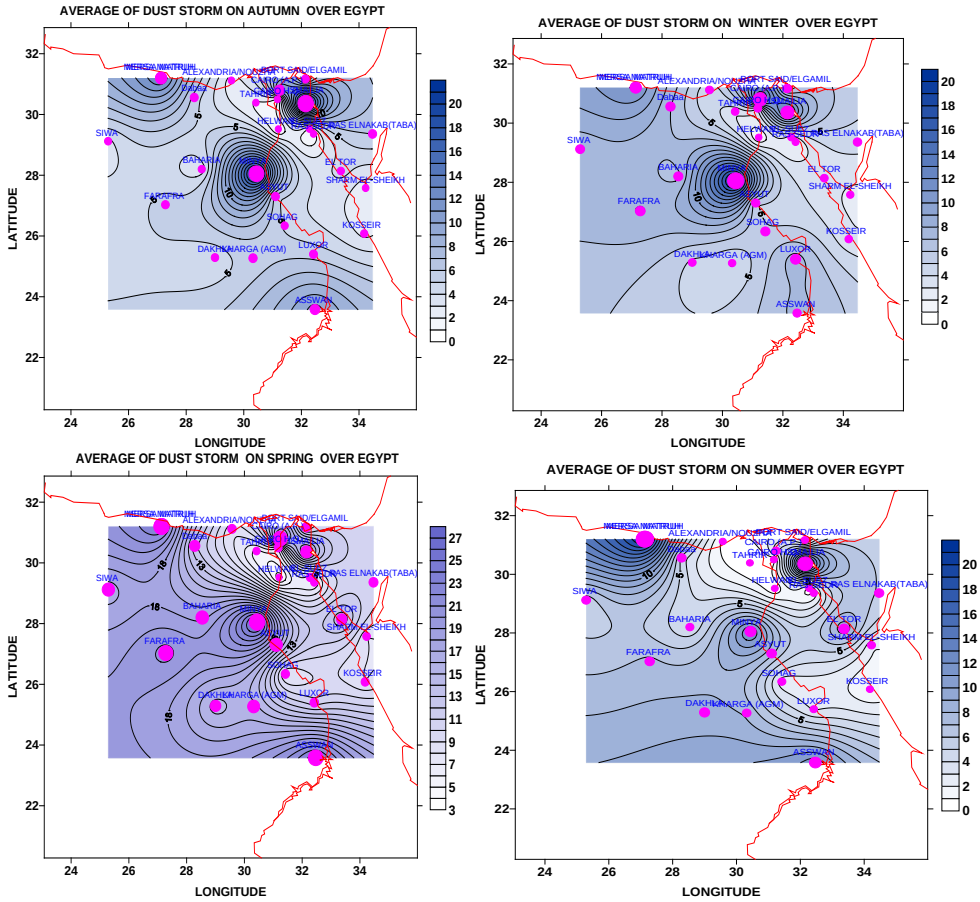

Fig.(4.9). The average season of dust storm on Egypt for 1968 to 2004

Fig (4.9) show the background aerosols are very large in spring season due to the impacts of the sand and dust storm events, the average of urban aerosol in autumn is larger than urban aerosol in the spring this due to the existence of an additional source for aerosols .summer in Egypt is almost dry season so there is no completely scavenging for aerosol and according to the accumulation of aerosols the background aerosols in autumn will be higher than in spring .

5- Changes in aerosol parameters during major dust storm events (2004–2005) over Cairo using AERONET and CIMEL

mineral dust and their properties, transport and dynamics .

Natural mineral dust aerosols and dust storms have attracted attention of scientists in the last few decades as they constitute one of the largest fractions of total aerosols transport and dynamics. Recently, dust aerosols have been found to influence the hydrologic cycle, monsoon system and climate as they are capable of changing radiative characteristics of the atmosphere ,there are some exceptions to this rule as is the case during the spring season when frequent chained depressions can be observed. These events, called ‘‘Khamsin’’ depressions in Arabic language, coincide with strong winds blowing from the south and raising dust on their way. Though the air masses associated with these events are warm and

relatively dry, occasional clouds, rainfall and thunderstorms may also be observed during these periods.

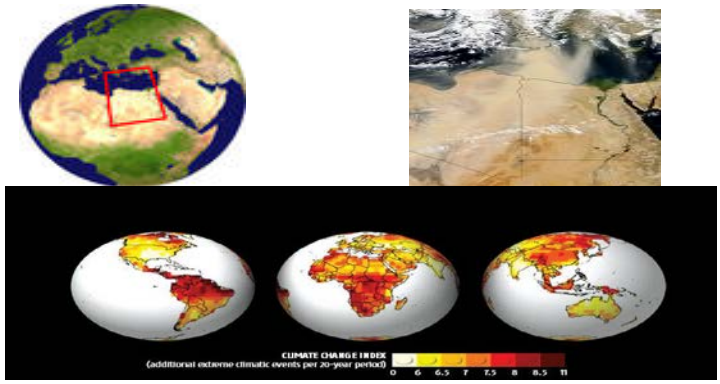

Figure 5-1. Aeronet images showing long range transport of dust storms. The white color represents clouds. The dust appears in pale beige color and Aeronet image per 20 year period

Dust storms originating from the arid and desert areas are found to be prime contributor of mineral dust throughout the world. The arid regions of Africa (Saharan Desert), Middle East, Arabian Desert, located several thousand kilometers upwind of the western side of the world [Gillette, 1999] and contribute a large fraction of mineral dust with respect to total annual loading. Recently, ground based Aerosol Robotic Network (AERONET) Fig (5-1), [Holben et al., 1998; Smirnov et al., 2000 ,and satellite data (Polarization and Directionality of the Earth's Reflectance's (POLDER), have been used extensively to study aerosol optical properties 2004-2005.

Aerosol loading is found to be highest during the spring season, March–may) and winter(Dec-Jan) because of large influx from long range transport of mineral dust aerosols from the western arid regions.

The air quality of the urban and rural areas lying along the track of dust storms changes significantly (size distribution and particulate matter concentrations) affecting health of people exposed during dust events [El-Askary et al., 2004 , 2006 Dey et al., 2004]. The real time monitoring and forecast of the dust storm events and their tracks will be useful in reducing exposure of these dust events to a large population (~ 70 million) living in the plains of Egypt.

Dust storms contribute largest fraction of aerosol optical depth (AOD) over Egypt during the khamsin period. Daily ground data (Aeronet) provide optical characterization of the dust for the whole seasons. For quantifying these effects an accurate determination of the aerosol properties is necessary.

We present physical properties and optical characterization of all major dust storm events occurred during the khamsin period 2004–2005(March– May) over Cairo where we focus in detail on the radical changes observed in aerosol optical properties(AOD, Angstrom exponent α, aerosol size distribution: ASD during dusty day for the year 2004-2005. Documenting these properties was one of the aims of Aeronet that has been carried out mainly in 2004 and 2005.

Among the many instruments implemented at various experimental sites, two Sun/sky radiometers (CIMEL) have been operated successively for more than 1 year (from 29 October 2004 to 31 January 2006). The first one was operated on the premises of Cairo University (Giza, 30°01'N, 31°12'E) until 14 April and was replaced afterward by another identical instrument operated at the Egyptian Meteorological Authority (EMA) headquarters located just a few kilometers away from the previous site (data collected at

these two sites (Cairo University and Cairo EMA, respectively) are available online at http://aeronet.gsfc.nasa.gov/) .
In this respect, efforts are being made currently to derive aerosol properties directly from satellite observations [Griggs, 1975; Holben et al., 1998; King et al., 1992]. Another approach also based on remote sensing consists in implementing a dense network of ground-based instruments from which key aerosol characteristics can be retrieved in quasi real time. This is the case of the Sun photometers deployed in the frame of the Aerosol Robotic Network (AERONET).

5 . Aerosol characteristics during spring campaign 2005

For the 2005 spring campaign we have performed a similar analysis. A general statistics is summarized in Table (4-1). Note that data in 2004-2005 range from October 2004 to april 2005, that is, the whole 2005 summer (April) Average AOD (440 nm) is 0.48 (STD 0.19); table (5-1) and most of the days in October to December 2004 have AOD (440 nm) above 0.2. and from Mars to July 2005 have AOD (440 nm) above 0.3 Very few observations (less than 2%) were below 0.2 for AOD (440 nm).

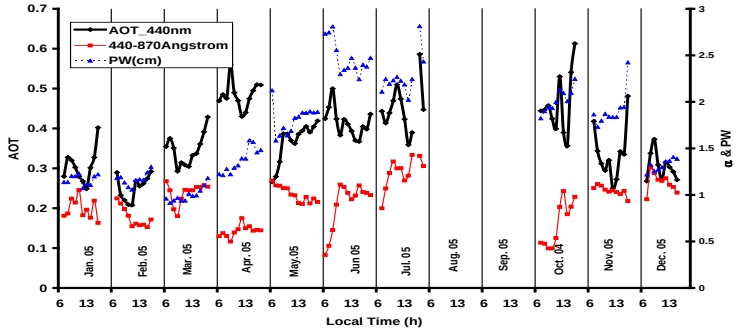

Fig. (5.4). AOD, alpha and PW during the 2004-2005 campaign

Months	AOD (440m)		Angstrom Exponent (440 –870 nm)		(PW)	
	Mean	Std. dev.	Mean	Std. dev.	Mean	Std. dev.
Oct.04	0.46	0.099	0.69	0.16	1.82	0.105
Nov.04	0.337	0.169	1.044	0.2337	1.908	0.40
Dec.04	0.3044	0.209	1.132	0.329	1.320	0.295
Jan.05	0.0566	0.1817	0.852	0.468	1.161	0.281
Feb.05	0.251	0.1024	0.759	0.346	1.167	0.298
Mar.05	0.345	0.1437	1.0238	0.4013	0.998	0.14
Apr.05	0.48	0.1959	0.6116	0.3421	1.367	0.342
May.05	0.366	0.1309	1.006	0.283	1.807	0.42
Jun.05	0.414	0.1337	0.895	0.299	2.475	0.387
Jul.05	0.450	0.125	1.237	0.243	2.269	0.320

Table 5-1. Monthly Averages and Associated SD of AOD Measured at Four Sun Photometer Wavelengths for Cairoa, Angstrom Exponent (440–870 nm) and PW During Year 2004-2005

"Data are for the period the period from 29 October 2004 to July 2005. The a values computed for several wavelength ranges and PW are also presented. Std, standard deviation; AOD, aerosol optical depths; PW, precipitable water."

The monthly averages of AOD at 440, 670, 870, and 1020 nm, α in different wavelength ranges, and PW during cloud-free days are listed in Table (5-1). Figure (5-4) shows a selection of these data, namely AOD at 440nm, α in the 440–870 nm wavelength range, and PW. The standard deviation of these quantities is visualized by the vertical bar associated with each monthly average. Figure (5-4) reveals significant month-to-month variation in AOD even though the amplitude of seasonal variations is rather limited when compared to the well-defined bell-shaped seasonal trend with maximum in summer which is usually observed in temperate climates [e.g., Iqbal, 1983; Gueymard and Garrison, 1998]. In Cairo, there are two marked AOD maximum in spring(March-May) and in winter in (December and January), are also observed. On the basis of this temporal pattern of AOD, which is in good agreement with previous results obtained by other authors [e.g., El-Wakil et al., 2001; Tadros et al., 2002; Zakey et al., 2004], four subperiods coinciding with the four seasons of the year can be defined for a more detailed temporal study of the aerosol characteristics in Cairo.

6. Characterization of the Aerosol Individual Components

Due to the pervasive presence of complex aerosol mixture in Egypt. there are often various combinations of both dominantly spherical shap particles (pollution)and distinctly non spherical particles characteristic of air borne soil dust. Since the particle size distributions determined by the angular distribution of sky radiances (and additionally from τ_a spectra). Components As detailed above, AOD method has allowed identification of at least two aerosol types in Cairo, namely dust-like and pollution-like aerosols, whose occasional presence in large concentration explains the observed large AOD values. Therefore, it is important to determine the characteristics of these single components in order to understand the variability of the aerosol characteristics over the city. The methodology chosen for achieving this goal has consisted in isolating in the data set the observations corresponding to periods when either the dust-like or the pollution-like types were clearly dominant and in averaging the products of the inversion scheme for these two sub data sets. Practically, the arbitrary numerical criteria selected for the separation of the two aerosol types have been derived from Figure (5.3): a dust-like component is assumed to be clearly dominant when AOD is larger than 0.5 and α is less than 0.5. Similarly, the pollution-like component is considered as dominating the aerosol properties when AOD is larger than 0.5 and α between 1 and 1.5. However, these definitions for the dust-like and pollution-like aerosols leave out a significant number of observations. Among them a first aerosol category with α values larger than 1.5 and whose importance is especially apparent in winter (Figure 5.3) can be defined. This particularly fine aerosol is also probably of anthropogenic origin and could be considered as constituting a background pollution aerosol type different from the ‘‘pollution type’’ previously defined. In summary, three main aerosol components have been identified: dust-like, pollution-like and background pollution. Table (5-1) summarizes the practical criteria used to separate the corresponding cases in the whole data set. It also provides the frequency of observations for each aerosol type. At this stage, it must be acknowledged that many observations, for instance all those yielding a values between 0.5 and 1.0, have not been considered as a single aerosol category. Indeed, these cases probably do not correspond to a single aerosol of unknown origin but rather to a mixing of the

previously identified dust, pollution, and background pollution components. Theoretically, one should be able to derive the physical characteristics of the overall (mixed) aerosol simply from the characteristics of the individual components and from the proportions of their mixture.

7. Volume Size Distributions

A flexible inversion algorithm, developed by Dubovik and King [2000] and modified by Dubovik et al. [2002b] can also be used to retrieve columnar aerosol characteristics from direct Sun and diffuse sky radiance measurements. These characteristics include the vertically averaged aerosol volume size distribution in a range of radii between 0.05 and 15 µm. This distribution v(r) is represented by a sum of n lognormally distributed populations:

$$v(r) = \frac{dV(r)}{d\ln r} = \sum_{i=1}^{n} \frac{C_{v,i}}{\sigma_i (2\pi)^{1/2}} \exp\left(-\frac{\left[\ln(r/r_{m,i})\right]^2}{2\sigma_i^2}\right), \quad (5\text{-}1)$$

in which v(r) and the amplitude of each population ($C_{V,i}$) are volume concentrations per cross section for an atmospheric column, r is the aerosol radius, $r_{m,i}$ is the volume geometric mean radius and σ_i is the geometric standard deviation for each mode. At each of the four wavelengths, the inversion procedure also provides the real and imaginary parts (n and k, respectively) of the aerosol complex refractive index (m).

The accuracy of the individual aerosol characteristics retrievals has been fully discussed by Dubovik et al. [2000, 228 2002a, 2002b, 2006]. It appears that one important source of uncertainty lies in the assumption made regarding the shape (spherical or spheroid) of the aerosol particles before running the inversion algorithm. For instance, in the presence of spheroid mineral dust particles the sphericity assumption leads to an over estimation of the finest classes in the inverted size distribution. It also creates an artificial spectral dependence of the real part of the refractive index and distortions in the retrieved phase function, especially at scattering angles larger than 80^o.A direct implication of the latter artifact is that g is also biased.

The spherical model is probably better adapted to both the pollution-like and background pollution components on the one side and the spheroid model more suitable for non spherical desert particles on the other side [Dubovik et al., 2006], the results discussed in this section will be those obtained with these respective assumptions. Another important point is that the particle size distribution retrieved from the inversion scheme and expressed by equation (5-1) have amplitudes terms (C_v) that increase with the amount of particles present in the atmospheric column, that is to say
the AOD. In consequence, the inverted size distributions have been normalized by the means of this AOD in order to facilitate comparison of the shapes of the three aerosol types' size distributions (Figure 5.5).

International Journal of Scientific Engineering and Applied Science (IJSEAS) – Volume-2, Issue-4, April 2016
ISSN: 2395-3470
www.ijseas.com

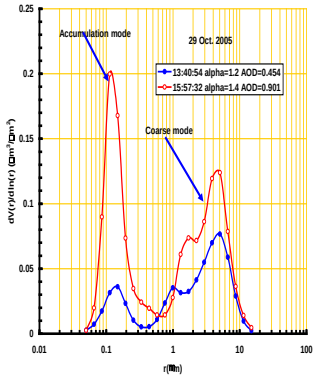

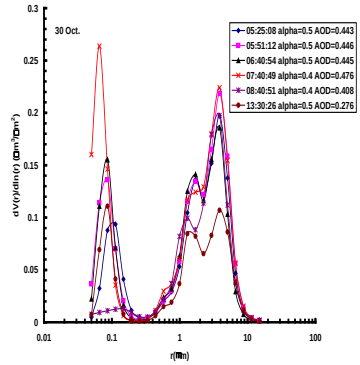

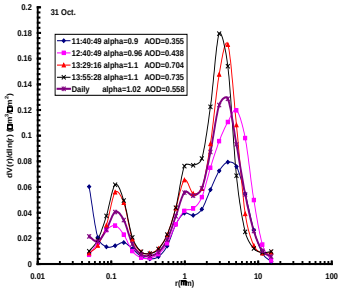

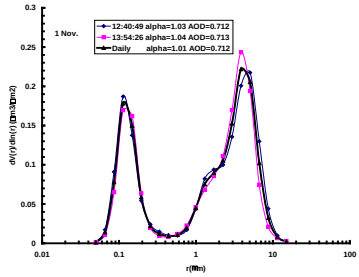

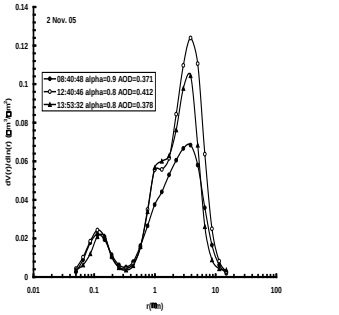

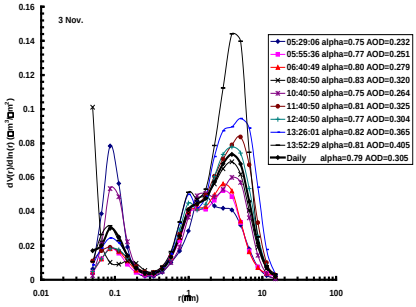

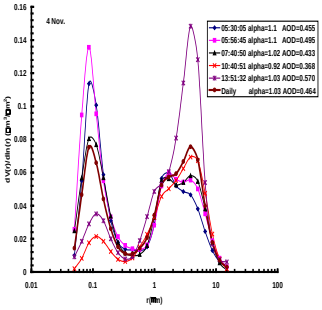

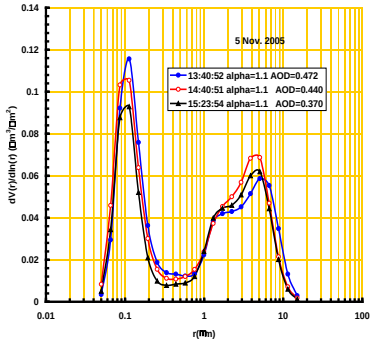

International Journal of Scientific Engineering and Applied Science (IJSEAS) – Volume-2, Issue-4, April 2016
ISSN: 2395-3470
www.ijseas.com

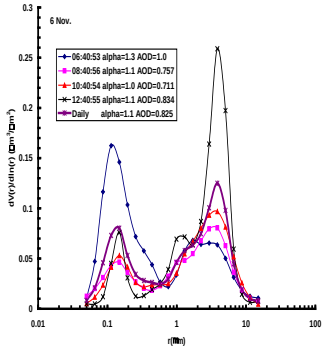

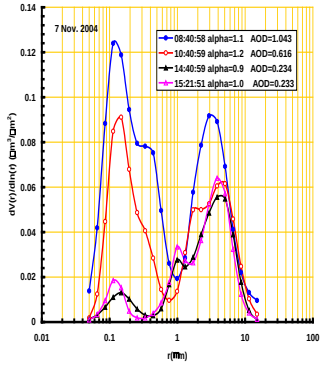

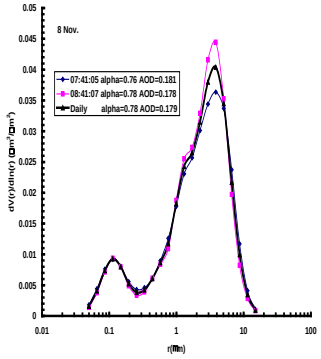

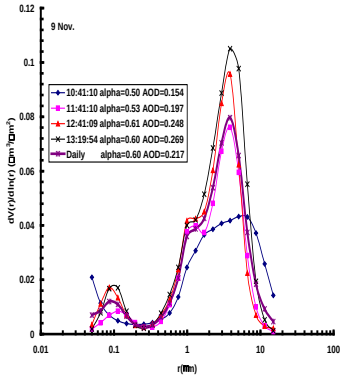

International Journal of Scientific Engineering and Applied Science (IJSEAS) – Volume-2, Issue-4, April 2016
ISSN: 2395-3470
www.ijseas.com

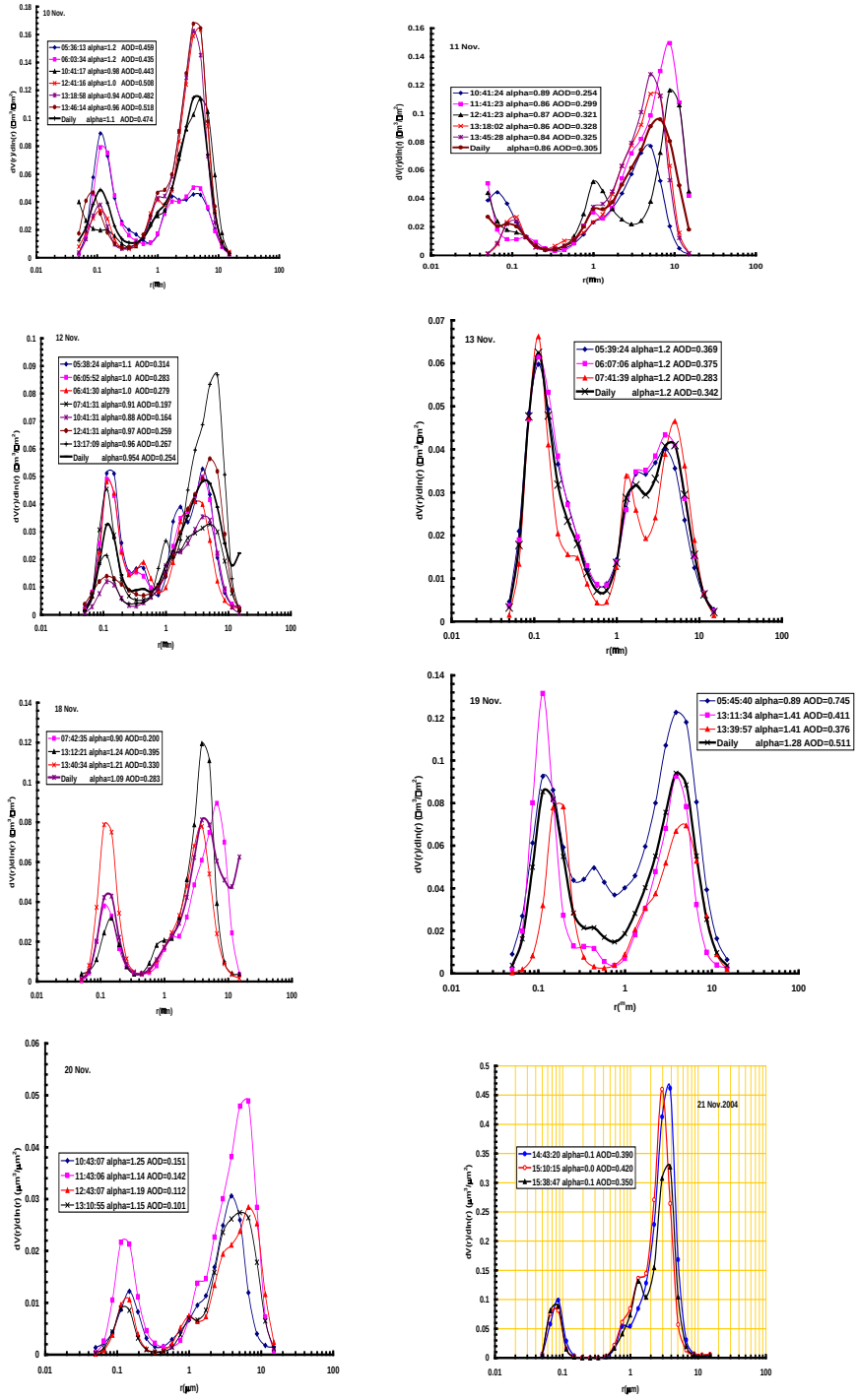

Figure (5.5). Aerosol size distributions of the three aerosol individual components normalized by the AOD.

The dust pollution and pollution-like aerosols (Figures (5.5) (29oct 2005 and4, 5,13 Nov) show the larger size fine mode particles at higher τ_a on a radius of 0.15 mm (± 0.03µm, SD) is likely due to increasing rates of coagulation as τ_a (and there concentration increases and also due to hygroscopic growth at higher R_H as a result of the presence of a dense motorized traffic within Cairo that releases very fine black carbon particles found of certain aerosol species such as sulfates which are produced in coal combustion. for the coarse mode ,there is no systematic trend in particle size as a function of τ_a, and mean maximum radius of the volume distribution is ~ 2.5µm, here there is large difference in the fine mode particles.

Table (5-2) Numerical Criteria Used for Separating Cases Dominated by the Three Aerosol Components (Dust, Pollution, and Background Mixed)

	AOD≥ 0.7		AOD < 0.7	
	Dust-Like	Pollution-Like	Background	Mixed
	$\alpha \leq 0.5$	$1 \leq \alpha \leq 1.5$	$\alpha \leq 1.5$	$\alpha < 1.5$
Frequency occurrences (%)	3	6	5	85

accumulation mode and of large industrial complexes around the city that, besides black carbon, indirectly produce large amounts of sulfate aerosols laying in the same size range [Seinfeld and Pandis, 1998; Abu-Allaban et al.,2002; Favez et al., submitted manuscript, 2007]. In addition to this, the fact that, except at diurnal and weekly scales for car traffic [Mahmoud et al., 2008], there is no significant temporal variation in these urban activities during the year could also explain that the background pollution aerosol is never associated with exceptionally large AOD values. This is not the case for the pollution-like aerosol whose emissions are particularly intense in autumn and whose origin has been assumed to be the biomass-burning process in the Nile delta. The size distribution obtained in this case is consistent with this assumption. Indeed, the burning of biomass is known to release at the same time particles in the accumulation mode (black carbon particles, mostly) but also coarser particles resulting from the condensation of organic compounds. As expected for wind mineral particles, the size distribution obtained in dust dominated conditions Figure (5.5) is characterized by the presence of a considerable amount of particles located in the super micron mode which coarse mode dominate case with similar τ_a=0.4 with less lower angstrom exponent α~0.4 .coarse particle mode associated with the predominantly fine mode τ_a cases shows little dynamic change as a function of τ_a . Contrary to what was observed with the two types of ‘‘pollution’’ aerosols, it clearly appears that the coarse mode itself is split in two different sub modes : one being centered on a radius of about 1.5 mm and the other at 4 mm. This bimodal structure of the coarse mode is similar to the one found during dust events by Eck et al .As a result, the parameters (C_v, r_m, σ) of the retrieved aerosol size distribution must be considered with caution when a significant amount of dust-like aerosol is present in the atmospheric column. In particular, the radius of the coarse particle mode yielded by the automatic inversion procedure is expected to be somewhere in between the values of the radii of the two real coarse particles sub modes, that is between 1.5 and 4 µm.

The ASD shows bimodal nature, with peaks in the range 0.5–10 and 0.05–0.5µm Figure (5.5)(30, 31Oct and 2,8,9,10,11,18,20 ,21 Nov). The moderate to coarse aerosol particles (0.5 –10 mm) show a large increase in the volume that indicate presence of moderate to coarse mineral dust particles because of the dust storms. The ASD peak is showing corresponding radius as well as its geometrical width and also show significant change in the characteristics of dust storm events over the plains with advance of the pre-monsoon season. time 13:30, 31Oct at 11:40 and 2 Nov at 8:40, 9 Nov at 10:41,10 Nov at the time 5

and 6, 20 Nov at the time10-12 , Figure(5.5) show bimodal size distribution with relatively large fraction of fine mode particles. Fraction of medium to coarse mode particles (~1-10μm) are found to gradually increase with increase in AOD due to dust events. The low Angstrom values (0-0.4) during dust events show the presence of coarse particles.

CONCLUSION

Analysis of the aerosol parameters retrieved over Egypt, situated in the central part, from ground-based AERONET (2004 – 2005) and satellite (MODIS) measurements show significant changes compared to non-dusty days prior to the dust storm events. Cairo AERONET data for all major dust storm events (year 2005) show large increase in AOD (τa500 nm) during event days (>1) and corresponding decrease in Angstrom exponent (a440 – 870 nm) showing presence of larger fraction of coarser particles which is also supported from ASD values. There is also increase in the intensity of dust storms (increase in maximum observed τa from >1 to >2.4 with advance of the khamasin condition) depending upon the source region and the travel path of dust storm. Significant change has been found in aerosol optical properties (ASD) during dust storm event days compared with non-dust days. The paired t-test shows that the dust storms change the aerosol optical properties (AOD) significantly. ASD also shows an increase in radius of maxima value from 1.71 to 2.24 mm implying presence of more coarse particles with advance of the khamsin condition. The weak spectral dependence of AOD for some of the dust events show the difference in the dust mineralogy of the dusts observed over the plains

The dissimilarities in the optical characteristics of the dust can be explained by change in characteristics during long range transport caused by mixing of mineral dust with dust from other regions (west Desert dust, soil dust), and mixing with anthropogenic aerosols over the plains.

One of the unique features of dust storms season is gradual rise of the aerosol loading with gradual increase in the intensity of dust storms with passage of the season (March–May). Increasing the dominance of mineral dust suppresses signature of anthropogenic aerosols and optical properties show more scattering signature. Absorbing aerosols are also found to be dominant during the winter season.